DOI: 10.1002/ejic.200600412

Morphology Control of CdSe Submicrostructures with High Hierarchy in Solution

Benxia Li,[a] Meng Jing,[a] Guoxin Rong,[a] Yang Xu,[a] and Yi Xie*[a]

Keywords: Morphology control / Cadmium selenide / Submicrostructures / Semiconductor

A series of CdSe submicrostructures, including rods, fringy structures, and fasciculate tubes with high hierarchy, have been selectively prepared by a facile one-step solution-based strategy without using any organic surfactants, simply by changing the feeding quantity of aqueous ammonia (25 % NH_3). The growth mechanism based on kinetic control is discussed for the selective formation of the CdSe submicrostructures with special morphologies. In the present reaction system, ammonia plays a dual role: providing an alkaline medium for the formation of Se^{2-} and acting as a coordinating agent for cadmium cations in either the solution or the solid phase. The feeding quantity of aqueous ammonia greatly influences the rate of formation of the Se^{2-} anion, and thus determines the final morphology of CdSe crystals. Compared with previous methods of preparing CdSe structures, this concise and novel one-step route has special advantages, suggesting a new path for convenient synthesis of CdSe materials with novel morphology.

Introduction

Recently, the synthesis of higher ordered functional materials with specific orientation, complex form, and hierarchy has been an area of active research.[1] More and more studies are focused on synthesizing one-dimensional (1D) nanostructures and their hierarchical assemblies, which are expected to play an important role in fabricating the next generation of microelectronic devices because they can function as both building units and interconnections.[2] The architectural control of functional materials with well-defined shapes between nanoscale and microscale is a key for the success of "bottom-up" approaches toward future microdevice fabrication.[3] In addition, the fabrication of semiconducting metal chalcogenides with micro- or nanosize has attracted intense interest because of the unusual optical and electrical properties of these compounds and their potential applications in microdevices.[4] CdSe is one of the most studied subjects because of its extensive applications in solar cells, luminescent materials, lasing materials, and biomedical imaging.[5] In the past several years, most of the studies on the synthesis of CdSe materials were focused on various 1D nanostructures[6] and tetrapod-branched nanocrystals.[7] Peng et al. have reported the shape control and size distributions of colloidal CdSe nanocrystals and proposed morphological evolution from 0D to 1D nanocrystals.[8] These studies were mostly focused on the synthesis of CdSe nanocrystals with diameters below 100 nm. Little attention was paid to the fabrication of submicro- or micrometer-sized CdSe materials with novel morphology. Recently, Zhang's group has demonstrated that the shapes of CdSe crystals with diameters of 150–1000 nm could be manipulated sequentially from rods to particles to tetrapod structures by a vapor-solid (VS) process at high temperatures.[9] Yet, the controllable synthesis of CdSe materials including 1D, quasi-1D, and 3D microstructures with high hierarchy through a direct low-temperature, solution-based route without the use of any organic additives or the aid of other techniques has been rarely reported.

Because of its easily controlled reaction conditions and facile manipulation, the solution-based route might provide an attractive option for large-scale production of micro- or nanomaterials with special morphology. In as-reported solution-based approaches for controlled synthesis of CdSe nanostructures, a curious feature of the systems has been the ubiquitous use of some organic additives as complexing agents or capping ligands.[10] For the purpose of property studies and future applications, it is desirable to develop convenient strategies to obtain new nanomaterials with desired shapes. Moreover, to meet the needs of designed synthesis of micro- or nanostructures with novel morphology, it is vital to systematically find experimental conditions under which the desired materials with controlled morphology are synthesized in large quantities. In this work, a series of CdSe submicrostructures, including rods, fringy structures, and fasciculate tubes, have been selectively prepared by a facile one-step solution-based strategy without using any

[a] Department of Nanomaterials and Nanochemistry, Hefei National Laboratory for Physical Sciences at Microscale, University of Science and Technology of China,
Hefei, Anhui 230026, P. R. China
Fax: +86-551-360-3987
E-mail: yxie@ustc.edu.cn
Supporting information for this article is available on the WWW under http://www.eurjic.org or from the author.

organic surfactants, by simply changing the feeding quantity of aqueous ammonia (25% NH_3). Concerning the use of ammonia in the synthetic architecture, a dual role can be identified: providing an alkaline medium for the formation of Se^{2-} anions and acting as a coordinating agent for cadmium cations in either solution or solid phase. This synthetic method provides a simple, environmentally friendly, and reproducible route for the controllable synthesis of CdSe materials.

Results and Discussion

Morphologies of the Products

The morphologies of the products obtained in the reaction systems containing different volume ratios of aqueous ammonia (25% NH_3) and distilled water were examined by a field-emission scanning electron microscope (FESEM). The FESEM images are shown in Figure 1. As shown in Figure 1 (a), the product obtained by feeding 20 mL aqueous ammonia (25% NH_3) was mainly composed of submicrorods with diameters around 500 nm and lengths ranging from 5 μm to 10 μm. When the volume of aqueous ammonia fed into the system was increased to 30 mL, fringy structures with high hierarchy assembled by nanorods was formed with about 85% morphological yield (Figure 1, b). A magnified SEM image in Figure 1 (c) clearly shows that the fringy assembly is formed by many smaller nanorods with diameters of 150 nm growing on a trunk. When aqueous ammonia (25%) was used as the only solvent, the obtained product was a large scale of 3D radial assemblies with an average diameter of about 5 μm, as depicted by the panoramic image (Figure 1, d). Interestingly, these 3D radial assemblies, different from those formed by aggregated nanorods that were reported previously,[11] are formed by fasciculate submicrotubes with diameters of 0.5–1 μm, and the open ends of some submicrotubes can be observed in Figure 1 (d). Parts e and f of Figure 1 show the magnified FESEM images of the assemblies with two representative shapes in the sample. The 3D assembly in Figure 1 (e) is composed of several thick tubes with diameters around 900 nm and wall thickness about 160 nm, which clearly manifests the tubular structure. The other assembly in Figure 1 (f) consists of more tubes with smaller diameters of 500 nm, in which these submicrotubes have cracked ends (arrowheads A) and rough interior walls (arrowhead B).

Phase and Composition of the Products

The structure and bulk phase of the products were determined by XRD analysis. Figure 2 shows the XRD patterns of as-obtained samples of submicron rods, fringy structures, and fasciculate tubes. All diffraction peaks in these XRD patterns can be well indexed to those of the pure phase of wurtzite CdSe (space group $P6_3mc$, JCPDS card No.2–330). No peaks due to impurities were detected, indicating the high purity of the product. The intense and sharp diffraction peaks suggest that the obtained products are well crystallized. In addition, it is notable that the intensity of {100} and {101} diffraction peaks is degressive and that of the

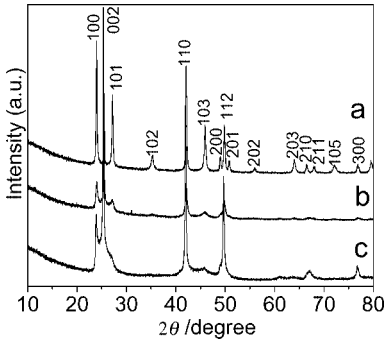

Figure 2. XRD patterns of three as-prepared CdSe samples: (a) submicrorods, (b) fringy structures, and (c) fasciculate submicrotubes.

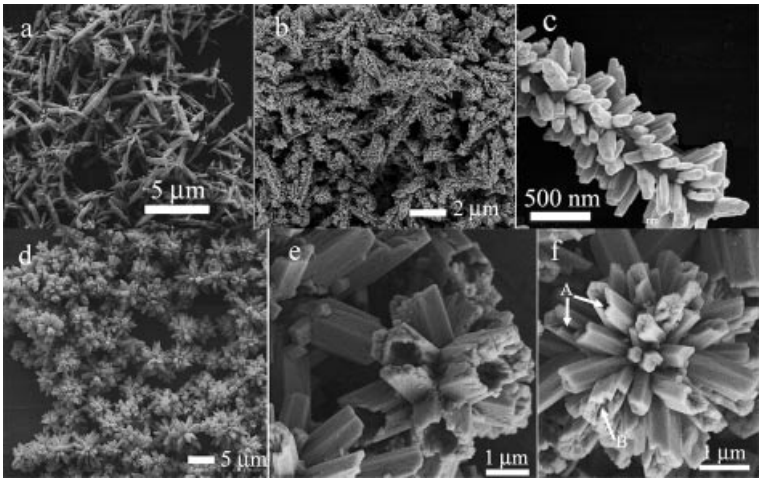

Figure 1. Typical FESEM images of three as-prepared CdSe samples with special morphologies by feeding different amounts of aqueous ammonia (25% NH_3): (a) submicrorods, 20 mL aqueous ammonia; (b–c) fringy structures, 30 mL aqueous ammonia; (d–f) fasciculate submicrotubes, 40 mL aqueous ammonia.

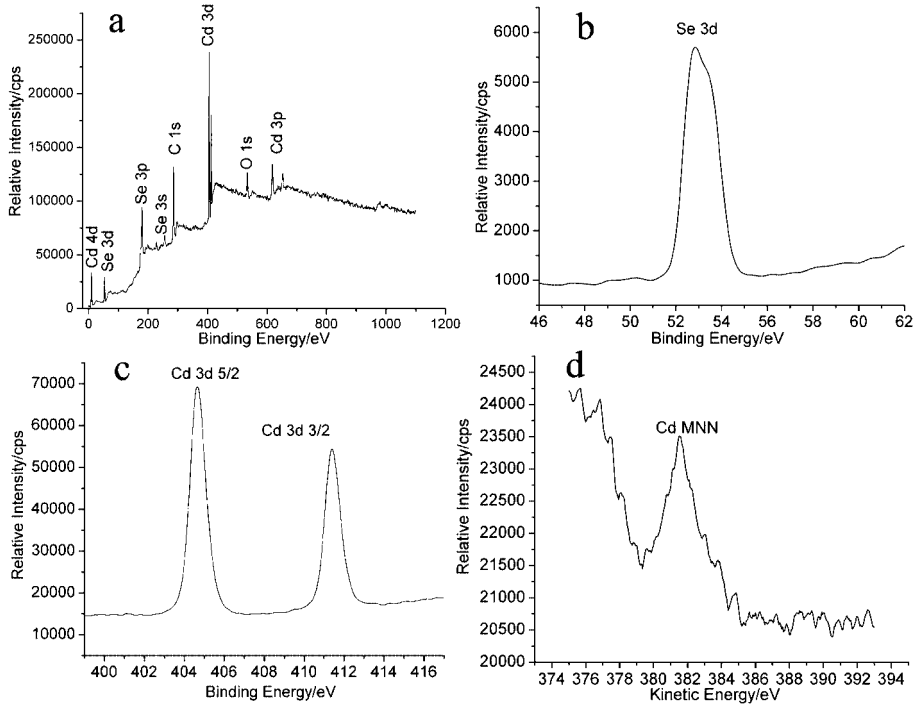

Figure 3. XPS spectra of the as-prepared CdSe fasciculate submicrotubes: (a) survey spectrum, (b) Se 3d, (c) Cd 3d, and (d) Cd MNN. The XPS spectra of other CdSe samples are similar.

{002} diffraction peak strengthens gradually from pattern a to pattern c, which results from the different arrangement of the rods in these CdSe submicrostructures. Thus, the XRD pattern can be indicative of the anisotropic shapes of the three CdSe samples.

In order to obtain the information about the electronic structure of the external ions and the relative composition of the product, three as-prepared CdSe samples with special morphologies were characterized by the XPS technique. Figure 3 shows the XPS spectra of CdSe fasciculate submicrotubes, in which the binding energies were corrected for specimen charging by referencing C 1s to 284.60 eV. The binding energies of Se 3d and Cd 3d were found to be 52.9 and 405.7 eV, respectively. The signals at 10.4 and 381.6 eV can be attributed to the binding energy of Cd 4d and the kinetic energy of Cd MNN. The Auger parameter, defined as the sum of the binding energy of the Cd 3d 5/2 level and the kinetic energy of Cd MNN, is approximately 786 eV, which is consistent with that of the CdSe material.[12]

Formation Process and Possible Mechanism of CdSe Submicrostructures

To better clarify the nucleation and anisotropic growth of these CdSe submicrocrystals, the morphology and microstructure of their intermediates were further studied by using transmission electron microscopy (TEM) and high-resolution transmission electron microscopy (HRTEM). As shown in Figure 4 (a), the 1-h reaction starting with 20 mL aqueous ammonia engendered very short CdSe rods with different diameters. After 5 h, well-shaped CdSe rods (Figure 4, b) had been formed. The electron diffraction (ED) (Figure 4, b1) and HRTEM image (Figure 4, b2) of a single CdSe rod in Figure 4 (b) indicate that the nanorod has a single-crystalline structure and grows along the <0001> direction. When 30 mL aqueous ammonia was fed into the system, the 1-h reaction gave primary CdSe fringy structures with fewer branches (Figure 4, c). After 5 h, the CdSe fringy structures (Figure 4, d) were almost achieved and resembled their corresponding final products. Figure 4d1 and Figure 4d2 show the ED pattern and HRTEM image taken from a branch (marked with a white rectangle) of the CdSe fringy structure in Figure 4 (d). The ED pattern can be indexed as the [100] zone axis of a wurtzite CdSe crystal, and the lattice spacings of 0.705 nm and 0.372 nm in the HRTEM image correspond to the (0001) and (01$\bar{1}$0) planes of hexagonal CdSe, respectively, indicating that the branches of the CdSe fringy structures grow along the <0001> direction. The ED pattern and HRTEM image of the trunk in the CdSe fringy structure are similar to those from the branch, indicating that the trunk of the CdSe fringy structures also grow along the <0001> direction. In addition, time-dependent experiments for the synthesis of the fasciculate submicrotubes were typically carried out to investigate the formation of the special tubular shapes. TEM images of the intermediate products are shown in Figure 4 (e–f). The 1-h reaction resulted in CdSe aggregations that consisted of many small whiskers (Figure 4, e). After 5 h, the whiskers grew into nanorods with diameters of 200 nm, and the aggregations became 3D radial architectures assembled by nanorods (Figure 4, f). The ED pattern (Figure 4, f1) and HRTEM image (Figure 4, f2), taken form the nanorod marked with a white rectangle in Figure 4 (f), indicate that the nanorods in CdSe are fasciculate crystal-

line nanorods that grow along the <0001> direction. The sample obtained after 12 h consists of larger 3D architectures assembled by nanorods, as revealed by its SEM images in Figure 5 (a–b). The magnified image of a typical architecture (Figure 5, b) indicates that the nanorods have very rough and cracked ends.

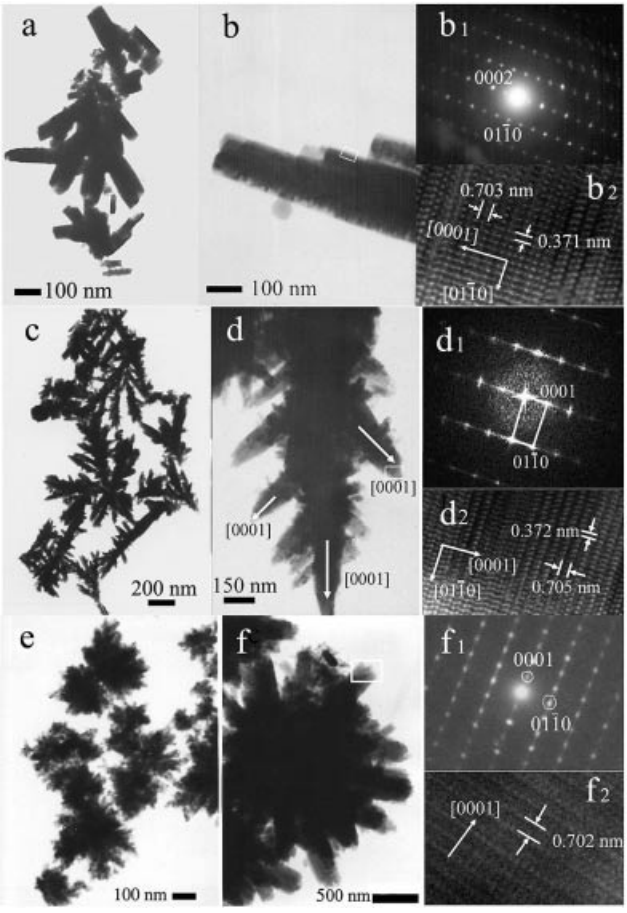

Figure 4. TEM images of the intermediate products of three CdSe submicrostructures: (a) rods obtained after 1 h; (b) rods obtained after 5 h, (b1,2) ED pattern and HRTEM image taken from the rod in Figure b; (c) fringy structure obtained after 1 h; (d) fringy structure obtained after 5 h; (d1,2) ED pattern and HRTEM image taken from the branch of the fringy structure in Figure d; (e) aggregations obtained after 1 h; (f) fasciculate rods obtained after 5 h, (f1,2) ED pattern and HRTEM image taken from the rod marked with a white rectangle in Figure f.

On the basis of the above experimental results, it can be seen that the most important factor that influences the morphology of CdSe crystals in the present approach is the concentration of ammonia in the reaction system. On one hand, our experimental results have indicated that the feeding quantity of aqueous ammonia (25%) in the reaction system also determined the composition of the final product (Figure S1–S2). Moreover, the presence of residual Se in the intermediate products (Figure S3) clarifies the formation process of the CdSe phase in the reaction, which can be illustrated by the series of reactions in Figure 6 (a): First,

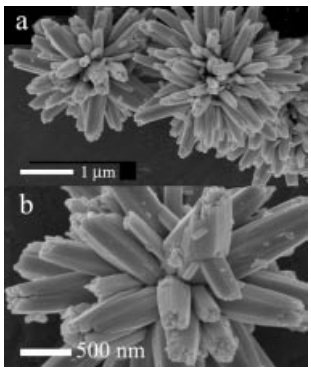

Figure 5. SEM images of CdSe fasciculate rods obtained after 12 h with using aqueous ammonia (25%) as the only solvent (40 mL).

SeO_3^{2-}, formed by the dissolution of SeO_2 in the solution, is reduced by $NaBH_4$ to Se. Then, under alkaline conditions, Se dismutates into Se^{2-} and SeO_3^{2-},[13] and the latter reacts again as the Se source. Finally, Se^{2-} anions combine with Cd^{2+} cations to form the CdSe phase. The formation of Se^{2-} anions needs proper alkaline conditions, provided by ammonia in our reaction system. On the other hand, it is well known that shape control of the crystals can be achieved by manipulating the growth kinetics.[14] In the present case, the contributing growth-driving force for CdSe crystals is primarily the Se^{2-} concentration, which is determined by the alkalinity of the reaction solution. In our reaction system, the alkalinity was manipulated by changing the feeding quantity of aqueous ammonia. The mechanism of formation of the CdSe submicrostructures with different morphologies is schematically described in Figure 6 (b). When the added volume of aqueous ammonia (25%) was as small as 20 mL, the alkalescence of the reaction solution was relatively weak, and the rate of formation of Se^{2-} anions was low, leading to a lower concentration in solution, which favored the anisotropic nucleation and growth of CdSe crystals. CdSe building units are inclined to grow along the <0001> axis because of the intrinsic structure of CdSe {0001} planes, where Cd^{2+} cations are rich on the positive facet (0001) and Se^{2-} anions are rich on the negative facet (000$\bar{1}$). Thus, one-dimensional nucleation and growth of CdSe nanorods along the <0001> axis took place, and the final CdSe submicrorods were obtained by feeding 20 mL aqueous ammonia (25%) into the present reaction system. With an increased volume of the aqueous ammonia (30 mL), both the alkalinity and the concentration of Se^{2-} anions in the reaction solution increased, giving more CdSe building units. Besides the one-dimensional growth, more nucleation sites around initial CdSe nanorods provided the growth along the <0001> direction of the new CdSe nanorods on the trunks. As a result, the fringy CdSe structures were obtained. When aqueous ammonia (25%) was used as the only solvent (40 mL), both the alkalinity and the concentration of Se^{2-} anions in the reaction solution increased further. The high monomer concentration led to a fast initial nucleation of CdSe, and many newly formed CdSe colloids aggregated together. Then, the concentration

of the monomer became lower as the reaction proceeded. The nuclei around the initial CdSe aggregations would grow along the <0001> direction to form 1D nanorods as long as the chemical environment constantly provides reactants. 3D-fasciculate submicrorods were obtained after 12 h. As for the CdSe fasciculate submicrotubes obtained in 40 mL aqueous ammonia (25%) after 24 h, it was deemed that they were formed by a coordination-assisted dissolution and recrystallization process.[15] Because Cd^{2+} cations are rich on the (0001) facet of the CdSe crystal, ammonia molecules tend to be adsorbed on the (0001) plane and coordinate with Cd^{2+} cations [$CdSe + 4\,NH_3 \rightarrow Cd(NH_3)_4^{2+} + Se^{2-}$], leading to the dissolution of solid CdSe. The selective adsorption of ammonia molecules on the tips [plane (0001)] of the CdSe rods would result in selective "etching" on the rods from the tips toward the interior along the <0001> axis. As observed from Figure 5 (b), the tips of these fasciculate rods are very rough and porous, which may be the "etching" effect of ammonia molecules. The transformation from the fasciculate nanorods to the fasciculate submicrotubes was achieved by partial dissolution of CdSe rods from the tips toward the interior along the long axis (<0001> axis). In addition, the diameters of the final tubes are larger than those of the rodlike precursors, indicating that recrystallization accompanied the "etching" process. Thus, final fasciculate submicrotubes were obtained through such a coordination-assisted dissolution and recrystallization process. However, in the rods and the fringy assemblies, obtained with 20 mL and 30 mL aqueous ammonia (25%), respectively, the CdSe crystals cannot adsorb enough ammonia molecules on their surfaces because of the low concentration of NH_3, and no tubular structures are formed in either system. Therefore, by adjusting the feeding quantity of aqueous ammonia, the morphology of the CdSe submicrostructures can be varied sequentially from 1D rods to 3D-fasciculate tubes.

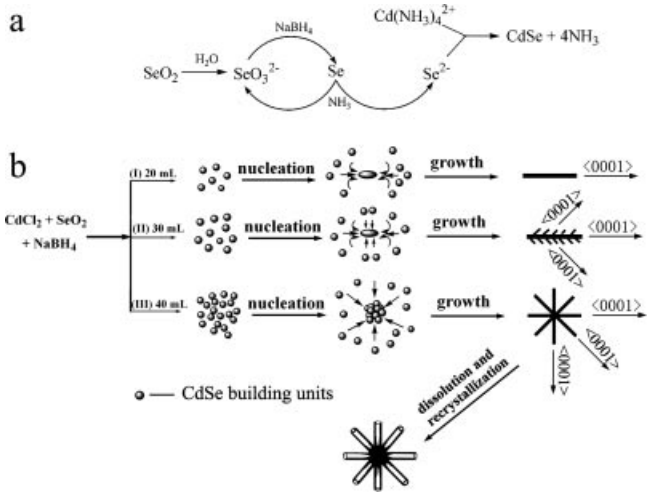

Figure 6. Schematic illustrations: (a) the formation process of CdSe phase in present reaction system; (b) the formation mechanism of CdSe submicrorods, fringy structures, and fasciculate tubes.

Conclusions

In summary, various morphologies of CdSe, including rods, fringy structures, and fasciculate tubes in submicroscale have been synthesized by a facile one-step, solution-based strategy without using any organic surfactants. The morphology of the CdSe submicrocrystals can be varied sequentially from rods to fringy structures and then to fasciculate tubes by manipulating the volume ratio of aqueous ammonia (25% NH_3) and distilled water. In the present reaction system, ammonia acts as a coordinating reagent as well as providing a suitable alkaline environment for the transformation from Se to Se^{2-}. The feeding quantity of aqueous ammonia greatly influenced the rate of formation of the Se^{2-} anion and thus its concentration in the reaction solution, which determined the final morphology of CdSe crystals. The rational mechanism based on kinetic control was discussed for the selective formation of these CdSe submicrocrystals with different morphologies. Compared with previous methods of preparing CdSe crystals, this concise one-step route has special advantages, which suggests a new path for the convenient synthesis of CdSe crystals with novel morphology.

Experimental Section

Materials and Preparation: All chemicals were of analytical grade and were used as received without further purification. In a typical procedure, $CdCl_2{\cdot}2.5H_2O$ (ca. 4 mmol), SeO_2 (ca. 4 mmol), and $NaBH_4$ (ca. 10 mmol) were dissolved in the solvent (40 mL) containing different volume ratios of aqueous ammonia (25% NH_3) and distilled water. The mixed solution was then transferred to a Teflon-lined autoclave with a total capacity of 50 mL. The autoclave was sealed and maintained at 180 °C for 24 h, and then cooled naturally to room temperature. The precipitates were carefully collected and washed with distilled water and absolute ethanol for several times, and then dried in vacuo at 60 °C for 4 h.

Characterization: XRD patterns of the products were obtained with a Japan Rigaku DMax-γA rotation anode X-ray diffractometer equipped with graphite-monochromatized Cu-K_α radiation (λ = 1.54178 Å). SEM images were taken with a field-emission scanning electron microscope (JEOL JSM-6700F, 15 kV). TEM photographs were taken with a Hitachi Model H-800 transmission electron microscope at an accelerating voltage of 200 kV. The HRTEM images and the corresponding SAED patterns were taken with a JEOL 2010 high-resolution TEM operating at 200 kV. The X-ray photoelectron spectra (XPS) were collected with an ESCALab MKII X-ray photoelectron spectrometer with non-monochromatized Mg-K_α X-ray as the excitation source.

Supporting Information (see also the footnote on the first page of this article): XRD patterns of the products obtained under different reaction conditions (Figure S1–S3), room-temperature photoluminescence (PL) emission spectra (Figure S4), and room-temperature Raman spectra (Figure S5).

Acknowledgments

This work was financially supported by the National Natural Science Foundation of China (No. 20321101). The authors thank Prof. Huagui Zheng for helpful discussions.

[1] a) H. T. Shi, L. M. Qi, J. M. Ma, N. Z. Wu, *Adv. Funct. Mater.* **2005**, *15*, 442–450; b) D. Wang, C. M. Lieber, *Nat. Mater.* **2003**, *2*, 355–356; c) G. F. Zou, K. Xiong, C. L. Jiang, H. Li, T. W. Li, J. Du, Y. T. Qian, *J. Phys. Chem. B* **2005**, *109*, 18356–18360.
[2] a) T. K. Sau, C. J. Murphy, *J. Am. Chem. Soc.* **2004**, *126*, 8648–8649; b) Z. R. Tian, J. Liu, J. A. Voigt, H. Xu, M. J. Mcdermott, *Nano Lett.* **2003**, *3*, 89–92; c) K. A. Dick, K. Deppert, M. W. Larsson, T. Martensson, W. Seifert, L. R. Wallenberg, L. Samuelson, *Nat. Mater.* **2004**, *3*, 380–384.
[3] X. Duan, Y. Huang, Y. Cui, J. Wang, C. M. Lieber, *Nature* **2001**, *409*, 66–69.
[4] a) T. C. Harman, P. J. Taylor, M. P. Walsh, B. E. LaForge, *Science* **2002**, *297*, 2229–2232; b) X. T. Zhang, Z. Liu, Q. Li, Y. Leung, K. Ip, S. K. Hark, *Adv. Mater.* **2005**, *17*, 1405–1410; c) I. Robel, B. A. Bunker, P. V. Kamat, *Adv. Mater.* **2005**, *17*, 2458–2463; d) S. C. Erwin, L. J. Zu, M. I. Haftel, A. L. Efros, T. A. Kennedy, D. J. Norris, *Nature* **2005**, *436*, 91–94.
[5] a) D. J. Milliron, A. P. Alivisatos, C. Pitois, C. Edder, J. M. J. Frechet, *Adv. Mater.* **2003**, *15*, 58–61; b) C. Ma, Y. Ding, D. F. Moore, X. Wang, Z. L. Wang, *J. Am. Chem. Soc.* **2004**, *126*, 708–709.
[6] a) W. Nie, L. J. An, B. Z. Jiang, X. L. Ji, *Chem. Lett.* **2004**, *33*, 836–837; b) C. Ma, Z. L. Wang, *Adv. Mater.* **2005**, *17*, 2635–2639.
[7] a) L. Manna, D. J. Milliron, A. Meisel, E. C. Scher, A. P. Alivisatos, *Nat. Mater.* **2003**, *2*, 382–385; b) J. W. Grebinski, K. L. Hull, J. Zhang, T. H. Kosel, M. Kuno, *Chem. Mater.* **2004**, *16*, 5260–5272; c) W. Nie, J. B. He, N. N. Zhao, X. L. Ji, *Nanotechnology* **2006**, *17*, 1146–1149.
[8] a) X. Peng, *Adv. Mater.* **2003**, *15*, 459–463; b) L. Qu, X. Peng, *J. Am. Chem. Soc.* **2002**, *124*, 2049–2055; c) Z. A. Peng, X. Peng, *J. Am. Chem. Soc.* **2001**, *123*, 1389–1395.
[9] Z. Y. Wang, Q. F. Lu, X. S. Fang, X. K. Tian, L. D. Zhang, *Adv. Funct. Mater.* **2006**, *16*, 661–667.
[10] a) Z. A. Peng, X. G. Peng, *J. Am. Chem. Soc.* **2001**, *123*, 1389–1395; b) C. R. Bullen, P. Mulvaney, *Nano Lett.* **2004**, *4*, 2303–2307; c) Q. Pang, L. J. Zhao, Y. Cai, D. P. Nguyen, N. Regnault, N. Wang, S. H. Yang, W. K. Ge, R. Ferreira, G. Bastard, J. N. Wang, *Chem. Mater.* **2005**, *17*, 5263–5267.
[11] a) Z. Q. Li, Y. Ding, Y. J. Xiong, Q. Yang, Y. Xie, *Chem. Eur. J.* **2004**, *10*, 5823–5828; b) C. Z. Wu, Y. Xie, D. Wang, J. Yang, T. W. Li, *J. Phys. Chem. B* **2003**, *107*, 13583–13587.
[12] C. D. Wagner in *Practical Surface Analysis Vol. 1: Auger and X-ray Photoelectron Spectroscopy* (Eds.: D. Briggs, M. P. Seah), John Wiley & Sons, Chichester, **1996**, 2nd ed., p. 595.
[13] a) W. X. Zhang, C. Wang, L. Zhang, X. M. Zhang, X. M. Liu, K. B. Tang, Y. T. Qian, *J. Solid State Chem.* **2000**, *151*, 241–244; b) W. X. Zhang, L. Zhang, Y. W. Cheng, Z. H. Hui, X. M. Zhang, Y. Xie, Y. T. Qian, *Mater. Res. Bull.* **2000**, *35*, 2009–2015.
[14] X. Peng, L. Manna, W. Yang, J. Wickham, E. Scher, A. Kadavanich, A. P. Alivisatos, *Nature* **2000**, *404*, 59–61.
[15] C. J. Jia, L. D. Sun, Z. G. Yan, L. P. You, F. Luo, X. D. Han, Y. C. Pang, Z. Zhang, C. H. Yan, *Angew. Chem. Int. Ed.* **2005**, *44*, 4328–4333.

Received: May 5, 2006
Published Online: September 13, 2006

